European Radiology (2019) 29:4239–4248
https://doi.org/10.1007/s00330-018-5990-1

COMPUTED TOMOGRAPHY

Initial exploration of coronary stent image subtraction using dual-layer spectral CT

Le Qin[1] · ShengJia Gu[1] · ChiHua Chen[1] · Huan Zhang[1] · ZhenBin Zhu[2] · XingBiao Chen[3] · Qun Han[3] · FuHua Yan[1] · WenJie Yang[1]

Received: 28 August 2018 / Revised: 11 December 2018 / Accepted: 19 December 2018 / Published online: 21 January 2019

Abstract

Objectives This study aimed to investigate the feasibility of coronary stent image subtraction using spectral tools derived from dual-layer spectral computed tomography (CT).

Methods Forty-three patients (65 stents) who underwent coronary CT angiography using dual-layer spectral CT were included. Conventional, 50-keV (kilo electron-volt), 100-keV, and virtual non-contrast (VNC) images were reconstructed from the same cardiac phase. Stents were subtracted on VNC images from conventional ($conv_{sub}$), 100-keV (100-keV_{sub}), and 50-keV (50-keV_{sub}) images. The in-stent lumen diameters were measured on subtraction, conventional, and 100-keV images. Subjective evaluation of reader confidence and subtractive quality was evaluated. Friedman tests were performed to compare in-stent lumen diameters and subjective evaluation among different images. Correlation between stent diameter and subjective evaluation was expressed as Spearman's rank correlation coefficient (r_s). The diagnostic accuracy was assessed according to invasive coronary angiography (ICA) performed in 11 patients (20 stents).

Results In-stent lumen diameters were significantly larger on subtraction images than those on conventional and 100-keV images ($p < 0.05$). Higher reader confidence was found on 100-keV, $conv_{sub}$, 100-keV_{sub}, and 50-keV_{sub} images compared with conventional images ($p < 0.05$). Subtractive quality of 100-keV_{sub} images was better than that of $conv_{sub}$ images ($p = 0.037$). A moderate-to-strong correlation between stent diameter and subjective evaluation was found ($r_s = 0.527$~0.790, $p < 0.05$). Higher specificity, positive predictive value, and negative predictive value of subtraction images were shown by ICA results.

Conclusions Subtraction images derived from dual-layer spectral CT enhanced in-stent lumen visibility and could potentially improve diagnostic performance for evaluating coronary stents.

Key Points

- *Dual-layer spectral CT enabled good subtractive quality of coronary stents without misregistration artifacts.*
- *Subtraction images could improve in-stent lumen visibility.*
- *Reader confidence and diagnostic performance were enhanced with subtraction images.*

Keywords Computed tomography angiography · Stents · Subtraction technique

✉ WenJie Yang
lisa_ywj@163.com

[1] Department of Radiology, Ruijin Hospital Affiliated to Shanghai Jiaotong University School of Medicine, No. 197 Ruijin 2nd Rd, Shanghai 200025, China

[2] Department of Cardiology, Ruijin Hospital Affiliated to Shanghai Jiaotong University School of Medicine, No. 197 Ruijin 2nd Rd, Shanghai 200025, China

[3] Philips Healthcare, A1, Lane 718, Lingshi Road, Shanghai 200233, China

Abbreviations

BMI	Body mass index
CCTA	Coronary computed tomography angiography
$CTDI_{vol}$	Volume of CT dose index
DLP	Dose length product
ECG	Electrocardiogram
ED	Effective dose
HR	Heart rate
HU	Hounsfield unit
ICA	Invasive coronary angiography
ICC	Intraclass correlation coefficient

ISR	In-stent restenosis
keV	Kilo electron-volt
NPV	Negative predictive value
PCI	Percutaneous coronary intervention
PPV	Positive predictive value
ROI	Region of interest
SEM	Standard error of measurement
VNC	Virtual non-contrast
WL	Window level
WW	Window width

Introduction

In recent years, percutaneous coronary intervention (PCI) has become an important treatment of choice for patients with coronary artery disease [1]. However, in-stent restenosis (ISR) is still the primary complication after PCI despite the introduction of drug-eluting stents [2, 3]. Although coronary computed tomography angiography (CCTA) has been increasingly performed noninvasively for evaluating ISR during the follow-ups, its clinical use is limited by "blooming artifacts" caused by beam hardening and partial volume effects [4]. Specially, CCTA is not appropriate for evaluating stents with a smaller diameter less than 3 mm or thick struts due to its lower diagnostic accuracy and underestimation of in-stent lumen [5–7]. In the last decade, generating subtraction images by subtracting non-contrast datasets from contrast-enhanced datasets to eliminate stents appeared to be one of the most promising approaches to improve in-stent lumen visualization and diagnostic accuracy [8, 9]. However, misregistration artifacts were inevitable because patients often could not withstand long-time breath-hold during the consecutive plain and enhanced scanning period.

Detector-based dual-layer spectral CT, which first came into commercial use in 2016, is characterized by a single x-ray source-detector system and achieves spectral separation at the detector level [10]. During spectral CT scanning, the dual layers of the detector absorb x-rays simultaneously, with the low-energetic spectrum in the upper layer and high-energetic photons in the deeper layer [11]. Therefore, a major advantage is the complete spatial and temporal alignment of the two datasets, which results in high spatial and temporal resolution for both virtual non-contrast (VNC) and monochromatic images [7]. So, it is supposed that these two traits have the potential to generate subtraction images without misregistration artifacts by subtracting VNC datasets from conventional and monochromatic datasets.

Hence, this study aimed to initially investigate the feasibility of coronary stent image subtraction using spectral tools derived from a dual-layer spectral CT and then determine whether the image quality and reader confidence of subtraction images would improve compared with corresponding routine images.

Materials and methods

Population

This study was approved by the Institutional Review Board of our institution and written informed consents were waived off due to the retrospective nature of the study. From January 2016 to September 2017, 90 consecutive patients with previous PCI (128 stents) examined using CCTA were included in the present study. Patients who underwent coronary artery bypass graft surgeries due to stent occlusion ($n = 6$) had no detailed information of stents provided ($n = 29$) or had severe vessel pulsatile artifacts ($n = 2$), and breathing motion artifacts on images ($n = 3$) were excluded. Those who had serial stents with an overlap of stent edges were also discarded to avoid measurements within the overlap zone of the stents ($n = 7$). A total of 43 patients (65 stents) were evaluated for the study.

CCTA examination

For patients whose heart rate (HR) ≥ 70 beats per minute (bpm), 50 mg oral beta-blockers (Metoprolol Tartaric Acid, AstraZeneca) were administered 45–60 min before CCTA examinations. All examinations were performed using a dual-layer spectral CT (IQon spectral CT, Philips Healthcare). All patients received intravenous contrast (Ultravist 370, Schering) via an 18-gauge catheter placed in the antecubital vein followed by saline. The injection protocol included an initial injection of 60-80 mL contrast at the rate of 5-6 mL/s according to the body mass index (BMI) followed by 30 mL of saline at the same rate. Scans were performed in the cranial-caudal direction during an inspiratory breath-hold with retrospective electrocardiogram (ECG)-gating. The bolus-tracking technique was used with a trigger threshold of 100 Hounsfield unit (HU) in the ascending aorta. The scanning parameters were as follows: voltage, 120 kVp; mAs, 500~620 mAs; collimation, 64×0.625 mm; pitch, 0.16; rotation time, 0.27 s; field of view, 257 mm; image matrix, 512×512; slice thickness, 0.9 mm; and slice increment, 0.45 mm. All images were reconstructed with filter of XCD for observing the stents specifically and then transferred to post-processing workstation (IntelliSpace Portal version 9.0, Philips Healthcare) for analysis.

Radiation dose

The volume of CT dose index ($CTDI_{vol}$, mGy) and dose length product (DLP, mGy × cm) were recorded from the exam summary page. The effective dose (ED, mSv) was estimated by multiplying DLP and a conversion factor for chest examination ($k = 0.014$ mSv × mGy^{-1} × cm^{-1}) [12].

Post-processing and data analysis

Conventional, 100-keV (kilo electron-volt), 50-keV, and VNC images of the same image range were extracted from one spectral-based image dataset in the same cardiac phase. Then, 100-keV images were set as high-energy images that reduced "blooming artifacts" without abating the visibility of the stent itself [13]. Further, 50-keV images were chosen as low-energy images, which were considered to be at the lowest energy level with a significantly lower image noise compared with 40-keV images [14]. Subtraction images were generated by subtracting stents on VNC images from conventional, 100-keV, and 50-keV images ($conv_{sub}$, 100-keV_{sub}, and 50-keV_{sub}) (Fig. 1).

At the mid portion of each stent on VNC image, a region of interest (ROI) within the stent was drawn as large as possible—avoiding in-stent lumen and adjacent adipose tissue—to calculate the CT attenuation of the stent. The "copy and paste" function was used to duplicate ROI on post-contrast (conventional and monochromatic) images so that the ROIs on all sets of images for each participant were seen in the same position. The ratio of CT attenuation between VNC images and post-contrast images was calculated using the CT value (HU): ratio = CT value (post-contrast)/CT value (VNC). When subtracting the images, two sets of images were sorted by *Z* position, and the weights of images were confirmed by their respective ratios to acquire the optimal subtractive effects because the subtraction function was based on CT values. The weight of post-contrast image was set as "1" and the weight of VNC image was set as "−ratio" to comply with the equation of CT values for stent "1 × post-contrast + (−ratio × VNC) = 0". Bias (HU) was also used to compensate the low CT values resulting from subtraction. That is, 1200–2200 HU on all tissues of subtraction images were added to make the attenuation of ascending aorta reach 350–450 HU. Thin straightened reconstruction images and curved plane reconstruction images along the long axis of stents were reconstructed for evaluation and measurement. Conventional and 100-keV images were observed with a fixed window level (WL) of 300 HU and a window width (WW) of 1200 HU, whereas WL and WW should be adjusted to optimize the demonstration of in-stent lumen when reading subtraction images.

In-stent lumen diameters of proximal, mid, and distal segments along the course of stents were measured by two senior radiologists with more than 5-year experience of cardiovascular diagnosis separately. The mean values of measurements from the two radiologists were taken for analysis. Reader confidence was rated on a 3-point scale based on the image quality: 1 point, conspicuous blooming artifacts, poor resolution and contrast, and totally non-diagnostic; 2 points, moderate blooming artifacts, moderate resolution and contrast, and partially diagnostic; and 3 points, little or no blooming artifacts, excellent resolution and contrast, and absolutely diagnostic. The criteria for evaluating the subtractive quality was based on a 5-point scale with respect to the removal of stents: 1 point, the stent was totally retained without any subtraction or the in-stent lumen was totally uninterpretable; 2 points, the stent was largely retained with very little subtraction or the in-stent lumen was poorly interpretable; 3 points, the stent was moderately subtracted and the in-stent lumen was fairly interpretable; 4 points, the stent was largely subtracted with very little remains, and the in-stent lumen was better interpretable; and 5 points, the stent was totally subtracted without any remains, and the in-stent lumen was fully interpretable. These scores were determined by the two aforementioned radiologists separately blinded to the detailed information of images. A third senior radiologist with more than 10-year experience in cardiovascular radiology was asked to make the final decision in the case of any disagreements to provide scores for further analysis.

Diagnostic accuracy

Eleven patients (20 stents) underwent invasive coronary angiography (ICA) within 30 days of CCTA examinations. Three patients underwent ICA for suspected ISR on conventional CCTA images, two for atypical chest pain but uncertain stent patency on CCTA, and the other six for atypical chest pain with patent stents but new significant coronary stenosis (> 50%) on CCTA. ICA was performed using standardized techniques by experienced cardiologists. At least two orthogonal projections were obtained for assessing target vessels. One expert observer blinded to CCTA data evaluated the stent patency as > 50% luminal diameter stenosis within the stent. The aforementioned two senior radiologists unaware of ICA findings evaluated ISR on CCTA images together.

Statistical analysis

The statistical analysis was performed on SPSS version 22.0 (IBM). All quantitative parameters were expressed as means ±

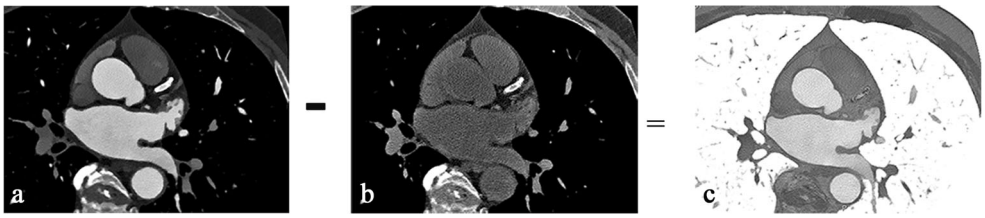

Fig. 1 Image subtraction. VNC image (**b**) subtracted from conventional images (**a**) gave subtraction images (**c**)

standard deviation (SD) or median and interquartiles (25th–75th percentiles), when appropriate. All qualitative parameters were reported as frequencies. The Kolmogorov–Smirnov tests were performed to test normal distribution, indicating that only 3 out of 15 sets of in-stent lumen diameter data were normally distributed. The Friedman tests were performed to compare in-stent lumen diameters and reader confidence among different groups of images. In the case of a statistically significant difference, post hoc pairwise comparisons using the Dunn–Bonferroni correction were performed. The inter-rater intraclass correlation coefficient (ICC) was used for inter-rater reliability analysis based on the alpha two-way random model. An ICC greater than 0.90, or between 0.75 and 0.90, or between 0.50 and 0.75, or less than 0.50 indicated excellent, or good, or moderate, or poor reliability, respectively. The inter-rater agreement for in-stent lumen diameter was assessed by the standard error of measurement (SEM), which was calculated by dividing SD of the mean differences between two measurements by $\sqrt{2}$ [15, 16]. The inter-rater agreement for the subjective image quality was estimated using kappa statistics. The scale for the kappa coefficient was defined as follows: less than 0.40, poor; 0.41–0.60, moderate; 0.61–0.80, good; and 0.81–1.00, excellent agreement. Correlations between stent diameter and subjective scores were expressed as Spearman's rank correlation coefficient (r_s). The correlation was considered poor if r_s was less than 0.4, moderate if r_s was 0.41–0.60, strong if r_s was 0.61–0.80, and very strong if r_s was greater than 0.81. For all analyses, p values less than 0.05 were regarded as statistically significant.

Table 1 Stent characteristics

Trade name (material)	Number
AVI (stainless steel 316L)	1
Excel (stainless steel 316L)	12
Firebird2 (cobalt-chromium alloy L605)	9
Firehawk (cobalt-chromium alloy L605)	3
Resolute (cobalt-nitinol MP35N)	27
Xience Prime (cobalt-chromium alloy L605)	11
Xience V (cobalt-chromium alloy L605)	1
Yinyi (stainless steel 316 L)	1
Stent location	
LM-LAD	2
LAD	29
D1	3
LCX	10
OM	1
RCA	20
Stent diameter (mm)	
2.25	5
2.5	14
2.75	11
3	15
3.5	13
4	7

LM left main, *LAD* left anterior descending, *D1* diagonal 1, *LCX* left circumflex, *OM* obtuse marginal, *RCA* right coronary artery

Results

A total of 43 patients with 65 stents were included in our study (mean age 65.7 ± 7.6 years old, range 48–83 years old; 26 males and 17 females; BMI 23.3 ± 7.1 kg/m^2; HR 64.1 ± 7.2 bpm, range 45–79 bpm). HR in six patients was still more than 70 bpm after administration of beta-blocker. Table 1 presents an overview of the characteristics of stents employed in the study. The stent nominal lumen diameter was 3.0 (2.5–3.5) mm. $CTDI_{vol}$ was 50.1 ± 7.3 mGy, DLP was 759.1 ± 128.5 mGy × cm, and estimated ED was 10.6 ± 1.8 mSv.

All image subtraction was successfully performed without misregistration artifacts. The ratio of CT values between post-contrast images and VNC images was 2.7 (2.1, 3.3), 1.8 (1.5, 2.4), and 4.8 (3.3, 6.1) for conventional, 100-keV, and 50-keV images, respectively. The ICC for all in-stent lumen diameters was 0.837–0.941 showing good and excellent reliability ($p < 0.05$). SEM for all in-stent lumen diameters was 0.08–0.11 mm representing a good agreement. The ICC showed a good-to-excellent reliability of 0.817–0.921 for reader confidence and a good reliability of 0.832–0.881 for the subtractive quality. The kappa coefficient revealed a good-to-excellent inter-rater agreement of 0.710–0.859 for reader confidence and a good agreement of 0.611–0.643 for the subtractive quality.

In-stent lumen diameters in $conv_{sub}$, 100-keV_{sub}, and 50-keV_{sub} images were much larger than those in conventional images and 100-keV images ($p < 0.05$) (Fig. 2). In addition, the in-stent lumen diameters of proximal and mid portions were larger in 50-keV_{sub} images than those in $conv_{sub}$ images. The reader confidence of 100-keV and subtraction images was much higher than that of conventional images ($p < 0.05$). Furthermore, with stents ≥ 3 mm in size, all subtraction images showed significantly larger in-stent lumen diameters compared with conventional images ($p < 0.05$). Besides, in-stent lumen diameters of 100-keV_{sub} and 50-keV_{sub} images were much larger than those of 100-keV images ($p < 0.05$). Only 100-keV and 100-keV_{sub} images demonstrated higher reader confidence compared with conventional images. Regarding stent size < 3 mm, all subtraction images revealed larger in-stent lumen diameters compared with conventional images, whereas 100-keV_{sub} and 50-keV_{sub} images revealed larger in-stent lumen diameters than 100-keV images did ($p < 0.05$). Moreover, the reader confidence of subtraction images was higher than that of conventional images ($p < 0.05$; Fig. 3). All the detailed

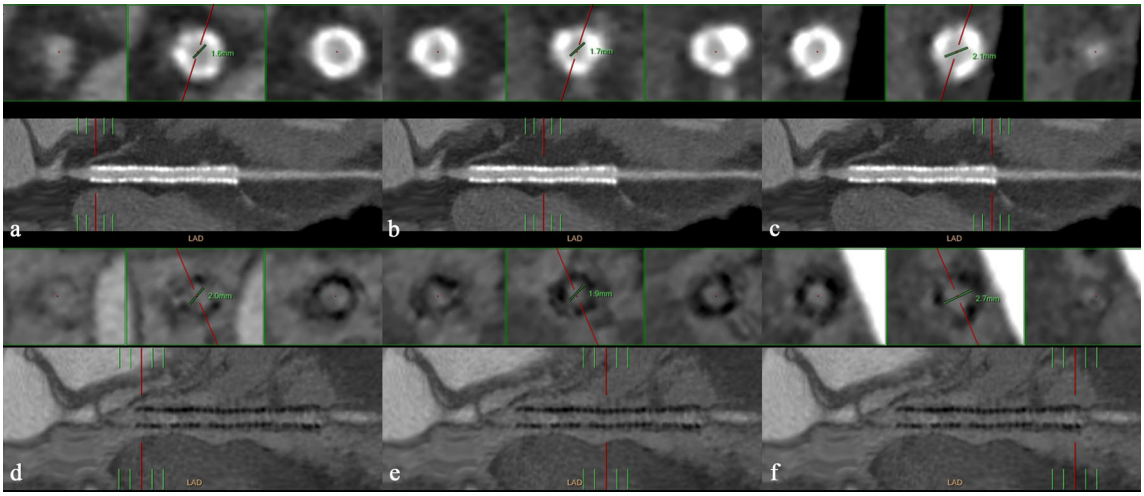

Fig. 2 Comparison of in-stent lumen diameter between conventional images and $conv_{sub}$ images. Thin straightened reconstructed images illustrated that the proximal, mid, and distal in-stent lumen diameter was larger on $conv_{sub}$ images (**d**–**f**) than on conventional images (**a**–**c**)

parameters of stent diameter and reader confidence are shown in Tables 2 and 3, respectively.

A total of 53 stents (81.5%), 57 stents (87.7%), and 55 stents (84.6%) were considered as 3 points or more of subtractive quality in $conv_{sub}$, 100-keV_{sub}, and 50-keV_{sub} images, respectively. The subtractive quality of 100-keV_{sub} images was higher than that of $conv_{sub}$ images ($p = 0.037$) (Fig. 4). Table 4 demonstrates a moderate-to-strong correlation between stent diameter and subjective evaluation of both reader confidence and subtractive quality ($p < 0.05$).

ICA showed that two stents were ISR in one patient with suspected ISR on CCTA and the other patient with the uncertainty of stent patency on CCTA. Table 5 demonstrates that non-assessable stents were reduced to none on subtraction images compared with conventional and 100-keV images. The specificity, positive predictive value (PPV), and negative predictive value (NPV) of subtraction images were higher than those of conventional and 100-keV images. Figure 5 shows an example illustrating the diagnostic performance of ISR using different series of images.

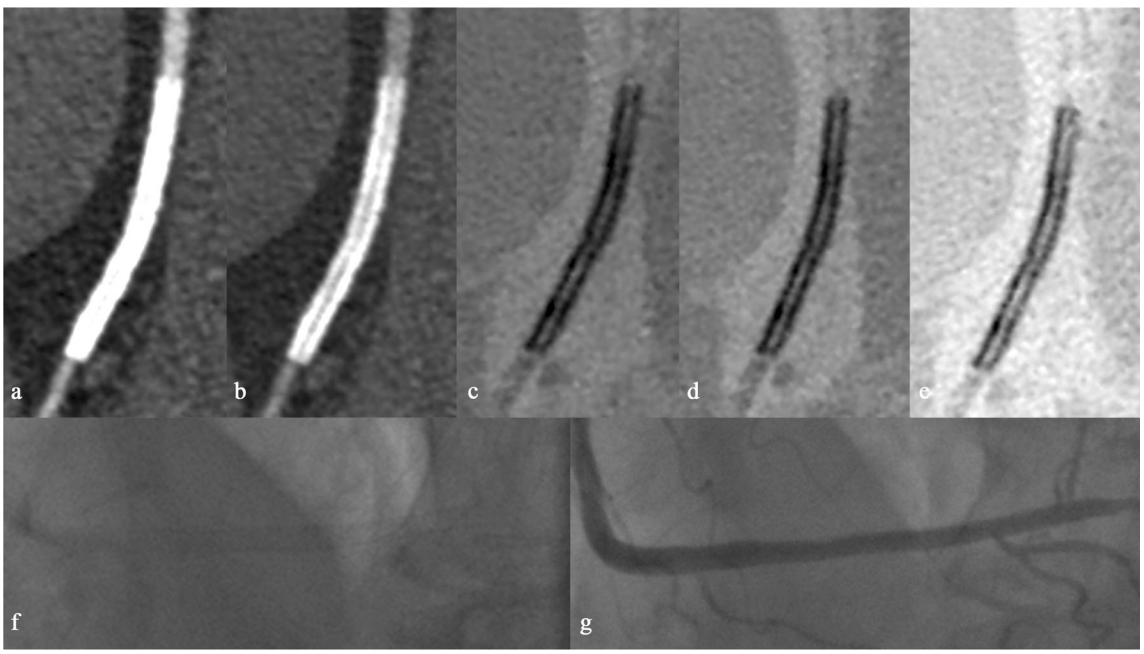

Fig. 3 A stent of 2.5 mm in diameter was implanted in distal right coronary artery (RCA). In-stent lumen patency was hard to diagnose on conventional (**a**) and 100-keV (**b**) images due to severe beam-hardening artifacts. After subtraction, $conv_{sub}$ (**c**), 100-keV_{sub} (**d**), and 50-keV_{sub} (**e**) images were interpretable and then the lumen patency was considered. The diagnosis was subsequently proved by ICA before (**f**) and after injecting contrast (**g**)

Table 2 Comparison of in-stent lumen diameter among conventional, 100-keV, and subtraction images by the Friedman tests and Dunn–Bonferroni tests for post hoc pairwise comparisons

	Conventional	100-keV	$Conv_{sub}$	100-keV_{sub}	50-keV_{sub}	*N*	*p* value
Overall							
Proximal stent (mm)	1.10 (0.80, 1.50)[b,c,d,e]	1.20 (0.88, 1.70)[a,c,d,e]	1.50 (1.15, 1.88)[a,b,e]	1.55 (1.20, 2.00)[a,b]	1.55 (1.28, 2.15)[a,b,c]	65	< 0.05
Mid stent (mm)	1.10 (0.70, 1.60)[b,c,d,e]	1.25 (0.83, 1.75)[a,c,d,e]	1.50 (1.10, 1.70)[a,b,e]	1.60 (1.20, 2.00)[a,b]	1.60 (1.23, 2.03)[a,b,c]	65	< 0.05
Distal stent (mm)	0.95 (0.68, 1.38)[b,c,d,e]	1.10 (0.78, 1.55)[a,c,d,e]	1.35 (1.00, 1.70)[a,b]	1.45 (1.10, 1.80)[a,b]	1.50 (1.10, 1.83)[a,b]	65	< 0.05
Stent diameter of 3 mm or more							
Proximal stent (mm)	1.45 (1.10, 1.70)[c,d,e]	1.60 (1.40, 1.90)[d,e]	1.80 (1.55, 2.30)[a,e]	2.00 (1.60, 2.40)[a,b]	2.00 (1.65, 2.50)[a,b,c]	35	< 0.05
Mid stent (mm)	1.55 (1.10, 1.75)[c,d,e]	1.60 (1.30, 2.05)[d,e]	1.75 (1.55, 2.30)[a]	1.90 (1.60, 2.45)[a,b]	1.85 (1.70, 2.35)[a,b]	35	< 0.05
Distal stent (mm)	1.30 (1.00, 1.70)[c,d,e]	1.50 (1.15, 1.80)[c,d,e]	1.65 (1.30, 2.20)[a,b]	1.80 (1.50, 2.20)[a,b]	1.80 (1.50, 2.30)[a,b]	35	< 0.05
Stent diameter less than 3 mm							
Proximal stent (mm)	0.78 (0.50, 1.00)[c,d,e]	0.85 (0.68, 1.10)[d,e]	1.20 (0.84, 1.41)[a]	1.20 (0.80, 1.46)[a,b]	1.30 (0.88, 1.45)[a,b]	30	< 0.05
Mid stent (mm)	0.70 (0.60, 1.00)[c,d,e]	0.80 (0.70, 1.10)[d,e]	1.05 (0.75, 1.40)[a]	1.20 (0.84, 1.40)[a,b]	1.23 (0.85, 1.41)[a,b]	30	< 0.05
Distal stent (mm)	0.68 (0.50, 0.81)[c,d,e]	0.75 (0.68, 0.91)[d,e]	1.00 (0.70, 1.36)[a]	1.15 (0.78, 1.40)[a,b]	1.10 (0.78, 1.41)[a,b]	30	< 0.05

In-stent lumen diameter was expressed as median (interquartiles)

[a] Statistical significance with conventional images

[b] Statistical significance with 100-keV images

[c] Statistical significance with $conv_{sub}$ images

[d] Statistical significance with100-keV_{sub} images

[e] Statistical significance with 50-keV_{sub} images

Discussion

The most significant finding of the present study was that detector-based spectral CT enabled coronary stent subtraction images without registration artifacts, thus improving the visualization of in-stent lumen and diagnostic performance. This novel study investigated the feasibility of coronary stent subtraction between VNC and monochromatic images derived from spectral CT.

Despite rapid advances in CT, it remains challenging to accurately evaluate the in-stent lumen by CCTA. Over the past few years, subtraction CCTA has emerged as a state-of-art technique with the potential to remove stents, allowing for a more accurate assessment of in-stent lumen. Amanuma et al reported significantly higher in-stent assessability and diagnostic accuracy for stent size ≤ 3 mm by subtraction [17]. One major limitation was that misregistration artifacts occurred between plain and contrast-enhanced scanning due to

Table 3 Comparison of reader confidence among conventional, 100-keV, and subtraction images by the Friedman tests and Dunn–Bonferroni tests for post hoc pairwise comparisons

	Point	Conventional	100-keV	$Conv_{sub}$	100-keV_{sub}	50-keV_{sub}	N	Post hoc	*p* value
Overall									
Reader confidence (*N* (%))	1	17 (26.2)	10 (15.4)	8 (12.3)	9 (13.8)	8 (12.3)	65	a vs b*	< 0.05
	2	34 (52.3)	23 (35.4)	27 (41.5)	17 (26.2)	18 (27.7)		a vs c*	
	3	14 (21.5)	32 (49.2)	30 (46.2)	39 (60)	39 (60)		a vs d*	
								a vs e*	
Stent diameter of 3 mm or more									
Reader confidence (*N* (%))	1	0 (0)	0 (0)	0 (0)	0 (0)	1 (2.8)	35	a vs b*	< 0.05
	2	21 (60)	5 (14.3)	14 (40)	5 (14.3)	5 (14.3)		a vs d*	
	3	14 (40)	30 (85.7)	21 (60)	30 (85.7)	29 (82.9)			
Stent diameter less than 3 mm									
Reader confidence (*N* (%))	1	17 (56.7)	10 (33.3)	8 (28.7)	9 (30)	7 (23.3)	30	a vs c*	< 0.05
	2	13 (43.3)	18 (60)	13 (43.3)	12 (40)	13 (43.3)		a vs d*	
	3	0 (0)	2 (6.7)	9 (30)	9 (30)	10 (33.4)		a vs e*	

a represents conventional images, *b*, represents 100-keV images, *c* represents $conv_{sub}$ images, *d* represents 100-keV_{sub} images, *e* represents 50-keV_{sub} images. *Represents statistical significance with $p < 0.05$

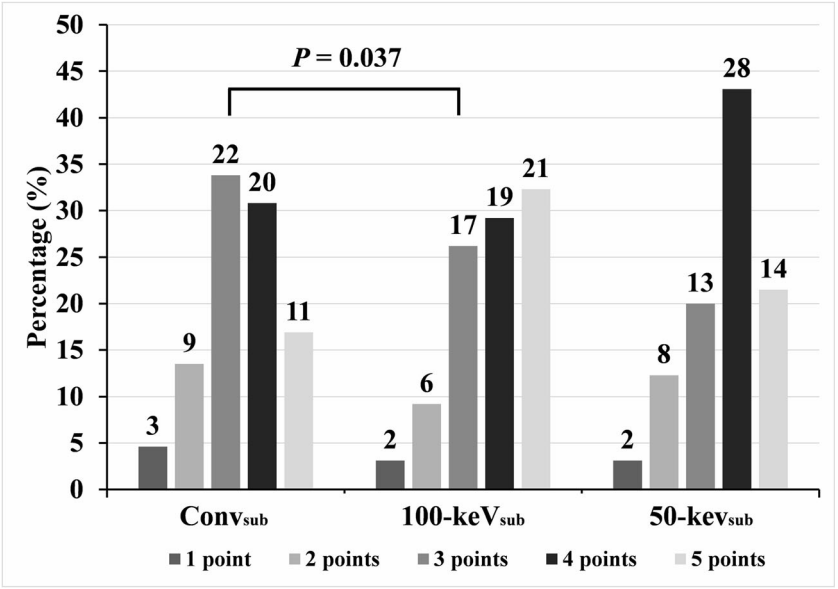

Fig. 4 Comparison of subtractive quality among $conv_{sub}$, 100-keV_{sub}, and 50-keV_{sub} images by the Friedman test and Dun-Bonferroni tests for post hoc pairwise comparisons. Significant difference of subtractive quality was found among three sets of images with 100keV_{sub} higher than $conv_{sub}$. The figures above the bars represent the amounts out of 65 sets of images

patient movement or various HR. Kidoh et al adopted a new method to get the first scan when the attenuation of ascending aorta arrived at 50 HU and get the second scan at the peak attenuation of ascending aorta, which led to a shorter breath-hold time and no misregistration artifacts [18]. However, only five patients were enrolled, and the breath-hold time remained relatively longer than that in the standard scanning protocol.

With the wide usage of dual-energy CT scanners, it is extremely reasonable to expect that subtraction between VNC images and monochromatic or mixed-energy images yielded equally improved in-stent lumen visibility and diagnostic accuracy without misregistration artifacts. By adopting this method, larger in-stent lumen diameters were measured on subtraction images, even compared with 100-keV images. Moreover, it was inferred that subtraction images rather than conventional images were appropriate to evaluate the in-stent lumen for the higher reader confidence in terms of stent size < 3 mm, which was deemed as inadequacies for CCTA. Interestingly, the in-stent lumen diameters and reader confidence of 50-keV_{sub} images seemed to be no less than those of $conv_{sub}$ and 100-keV_{sub} images, although the low-energy images were commonly thought to have poor visibility for the severe blooming artifacts [19]. This was because the stents could be completely subtracted according to the ratio of CT attenuation between VNC and 50-keV images. Another reason might be the high image quality of 50-keV images generated by dual-layer spectral CT: approximately constant image noise for monochromatic images that ranged from 50 to 200 keV, high contrast-noise rate at 50 keV, and reduced beam-hardening artifacts for monochromatic images via raw data based spectral reconstruction [20].

In addition, the present study showed that the stent diameter had a positive correlation with the subtraction quality. It was supposed that for stents with a smaller caliber, one voxel might contain both stent and iodine, which was hard for the following material decomposition, due to partial volume effects of CT. This was similar to the study by Moon et al in which smaller urinary stones would not be differentiated from iodine and were invisible on VNC images [21]. Furthermore, subtraction images showed some improvement in diagnostic accuracy and less non-assessable stents compared with conventional images and 100-keV images.

One of the most superior advantages of dual-layer spectral CT was that the misregistration artifacts were totally eliminated because the VNC and post-contrast images were generated from one dataset in the same cardiac phase. However, a major challenge was that the attenuation of stents on conventional, 100-keV, and 50-keV images was higher than that on VNC

Table 4 Correlation between stent diameter and subjective evaluation expressed as Spearman's rank correlation coefficient

	r_s	p value
Reader confidence		
Conventional image	0.773	< 0.05
100-keV image	0.790	< 0.05
$Conv_{sub}$ image	0.527	< 0.05
100-keV_{sub} image	0.676	< 0.05
50-keV_{sub} image	0.595	< 0.05
Subtraction quality		
$Conv_{sub}$ image	0.599	< 0.05
100-keV_{sub} image	0.530	< 0.05
50-keV_{sub} image	0.539	< 0.05

r_s Spearman's rank correlation coefficient

Table 5 Diagnostic accuracy of different sets of images in 11 patients (20 stents)

	Conventional	100-keV	$Conv_{sub}$	100-keV_{sub}	50-keV_{sub}
Non-assessable	4	2	0	0	0
Sensitivity (%)	50	50	50	50	50
Specificity (%)	66.7	83.3	88.9	94.4	94.4
PPV (%)	14.3	25	33.3	50	50
NPV (%)	92.3	93.8	94.1	94.4	94.4

images. Hence, further adjustment was needed to perform subtraction. Such a difference might be due to the fact that VNC was derived from a two-material decomposition algorithm which was designed to separate between iodine and soft tissue [6]. The atomic number of chemical elements in stents was much closer to that of iodine, which would not demonstrate a neat separation between stent and iodine contrast agent within in-stent lumen [22]. Consequently, a portion of stent was eliminated from VNC images because iodine caused the lower CT attenuation of stent on VNC images. Another possibility might be that beam hardening from both stent and contrast medium would alter the CT values because the stent was adjacent to the contrast medium, thus deteriorating the VNC quality [23]. This meant that the weights of the two sets of images should be adjusted according to the ratio for complete subtraction. The validity of this method was proved by the result that a majority of stents (81.5~87.7%) had a moderate-to-excellent subtractive quality.

This study had some limitations. Above all, a retrospectively instead of a prospectively ECG-gated method was performed in this study, leading to a relatively high radiation dose. Many studies suggested that prospectively ECG-gated CCTA could provide the image quality comparable to that for the retrospectively gated technique with much lower radiation dose [24, 25]. However, the reason for using retrospectively gated scanning was that IQON CT was a 64-multislice scanner with relatively low time resolution for patients with HR > 70 bpm. For patients with low HR, prospective ECG-triggered CCTA would require extended scanning time, longer breath-holding time, and increased contrast medium volume, which were more likely to result in streak

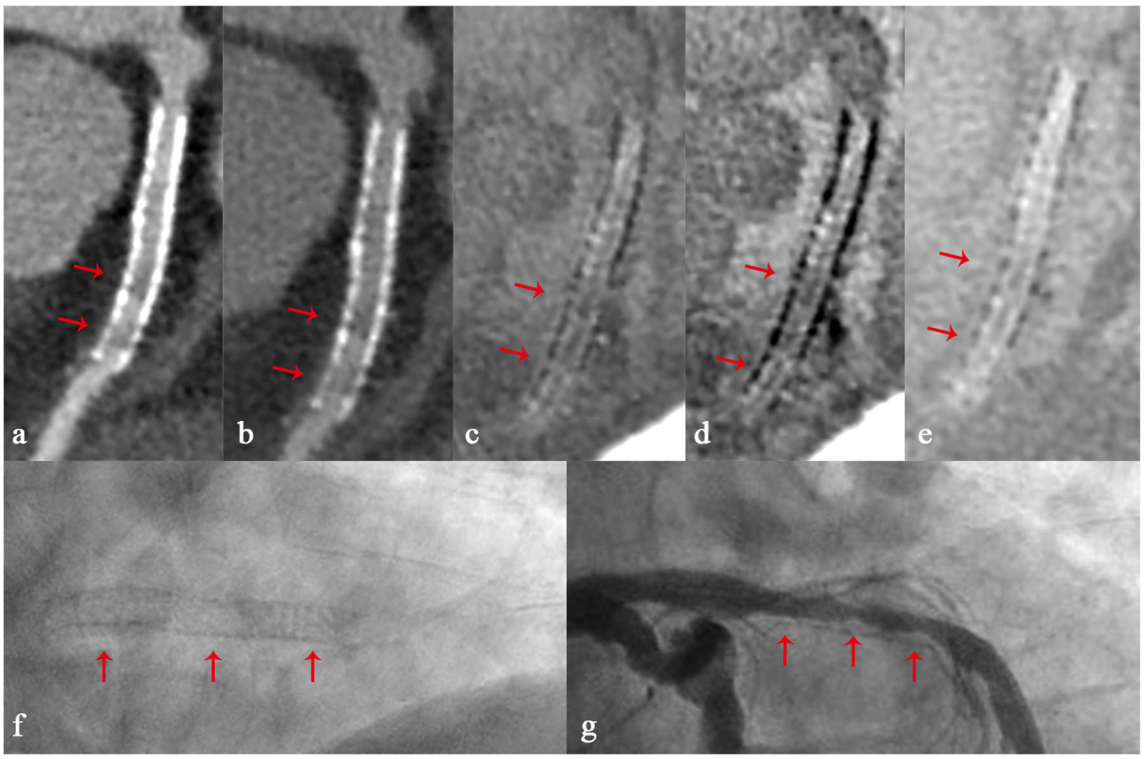

Fig. 5 A stent of 3.5 mm in diameter was implanted in proximal left anterior descending (LAD) artery. Conventional (**a**) and 100-keV (**b**) images displayed the hypo-attenuation within the in-stent lumen suspected of ISR. $Conv_{sub}$ (**c**), 100-keV_{sub} (**d**), and 50-keV_{sub} (**e**) images also revealed the presence of ISR, which was affirmed by ISR. Corresponding ICA images before (**f**) and after injection (**g**) demonstrated severe narrowing within the stent lumen. Red arrows represent the position of stent and ISR

artifacts of stents and more unassessable stents [26]. Moreover, the diagnostic performance of subtraction images should be interpreted with caution and further verified in a larger number of patients to avoid a risk of referral bias. The majority of patients receiving ICA in this study tended to have ISR or stent patency but new significant coronary artery stenosis on CCTA. This was because ICA was an invasive modality, but not a routine post-procedural tool for patients after PCI unless ISR was strongly suspected. Finally, subtraction images should be interpreted with conventional images as complements rather than diagnostic CT images solely because the visualization of primary vessels might be suboptimal.

In conclusion, subtraction between VNC and conventional or monochromatic images was achieved successfully in coronary stents by dual-layer spectral CT without misregistration artifacts. Further, subtraction CCTA images derived from dual-layer spectral CT enhanced in-stent lumen visibility and could potentially improve diagnostic performance, providing new insights into the evaluation of coronary stents.

Acknowledgements The authors thank Baisong Wang, PhD, a statistic teacher at Shanghai JiaoTong University, for providing statistical analysis. We also thank Yan Jiang and JianQing Sun for their great technical support.

Funding The authors state that this work has not received any funding.

Compliance with ethical standards

Guarantor The scientific guarantor of this publication is WenJie Yang.

Conflict of interest The authors of this manuscript declare no relationships with any companies whose products or services may be related to the subject matter of the article.

Statistics and biometry No complex statistical methods were necessary for this paper.

Informed consent Written informed consent was waived by the Institutional Review Board.

Ethical approval Institutional Review Board approval was obtained.

Methodology
- retrospective
- cross-sectional study
- performed at one institution

References

1. André F, Korosoglou G, Hosch W et al (2013) Performance of dual source versus 256-slice multi-slice CT in the evaluation of 16 coronary artery stents. Eur J Radiol 82:601–607
2. Maintz D, Burg MC, Seifarth H et al (2008) Update on multidetector coronary CT angiography of coronary stents: in vitro evaluation of 29 different stent types with dual-source CT. Eur Radiol 19:42–49
3. Ebersberger U, Tricarico F, Schoepf UJ et al (2013) CT evaluation of coronary artery stents with iterative image reconstruction: improvements in image quality and potential for radiation dose reduction. Eur Radiol 23:125–132
4. Stehli J, Fuchs TA, Singer A et al (2015) First experience with single-source, dual-energy CCTA for monochromatic stent imaging. Eur Heart J Cardiovasc Imaging 16:507–512
5. Alani A, Nakanishi R, Budoff MJ (2014) Recent improvement in coronary computed tomography angiography diagnostic accuracy. Clin Cardiol 37:428–433
6. Kalisz K, Halliburton S, Abbara S et al (2017) Update on cardiovascular applications of multienergy CT. Radiographics 37:1955–1974
7. Rajiah P, Rong R, Martinez-Rios C, Rassouli N, Landeras L (2017) Benefit and clinical significance of retrospectively obtained spectral data with a novel detector-based spectral computed tomography - initial experiences and results. Clin Imaging 49:65–72
8. Fuchs A, Kühl JT, Chen MY et al (2015) Feasibility of coronary calcium and stent image subtraction using 320-detector row CT angiography. J Cardiovasc Comput Tomogr 9:393–398
9. Yamaguchi T, Ichikawa K, Takahashi D, Sugaya T, Furuya J, Igarashi K (2017) A new contrast enhancement protocol for subtraction coronary computed tomography requiring a short breath-holding time. Acad Radiol 24:38–44
10. Ananthakrishnan L, Rajiah P, Ahn R et al (2017) Spectral detector CT-derived virtual non-contrast images: comparison of attenuation values with unenhanced CT. Abdom Radiol (NY) 42:702–709
11. Hickethier T, Baeßler B, Kroeger JR et al (2017) Monoenergetic reconstructions for imaging of coronary artery stents using spectral detector CT: in-vitro experience and comparison to conventional images. J Cardiovasc Comput Tomogr 11:33–39
12. American Association of Physicists in Medicine (2008) The measurement, reporting, and management of radiation dose in CT: report of AAPM task group 23 of the diagnostic imaging council CT committee. Technical report, College Park, MD: AAPM, 2008: AAPM report 96
13. Mangold S, Cannaó PM, Schoepf UJ et al (2016) Impact of an advanced image-based monoenergetic reconstruction algorithm on coronary stent visualization using third generation dual-source dual-energy CT: a phantom study. Eur Radiol 26:1871–1878
14. Ehn S, Sellerer T, Muenzel D et al (2018) Assessment of quantification accuracy and image quality of a full-body dual-layer spectral CT system. J Appl Clin Med Phys 19:204–217
15. de Vet HC, Terwee CB, Knol DL, Bouter LM (2006) When to use agreement versus reliability measures. J Clin Epidemiol 59:1033–1039
16. Kottner J, Audigé L, Brorson S et al (2011) Guidelines for reporting reliability and agreement studies (GRRAS) were proposed. J Clin Epidemiol 64:96–106
17. Amanuma M, Kondo T, Sano T et al (2016) Assessment of coronary in-stent restenosis: value of subtraction coronary computed tomography angiography. Int J Cardiovasc Imaging 32:661–670
18. Kidoh M, Utsunomiya D, Oda S et al (2015) Optimized subtraction coronary CT angiography protocol for clinical use with short breath-holding time-initial experience. Acad Radiol 22:117–120
19. Halpern EJ, Halpern DJ, Yanof JH et al (2009) Is coronary stent assessment improved with spectral analysis of dual energy CT? Acad Radiol 16:1241–1250
20. Ozguner O, Dhanantwari A, Halliburton S, Wen G, Utrup S, Jordan D (2018) Objective image characterization of a spectral CT scanner with dual-layer detector. Phys Med Biol 63:025027
21. Moon JW, Park BK, Kim CK, Park SY (2012) Evaluation of virtual unenhanced CT obtained from dual-energy CT urography for detecting urinary stones. Br J Radiol 85:e176–e181

22. Patino M, Prochowski A, Agrawal MD et al (2016) Material separation using dual-energy CT: current and emerging applications. Radiographics 36:1087–1105
23. Mangold S, Thomas C, Fenchel M et al (2012) Virtual nonenhanced dual-energy CT urography with tin-filter technology determinants of detection of urinary calculi in the renal collecting system. Radiology 264:119–125
24. Esposito A, Colantoni C, De Cobelli F et al (2013) Multidetector computed tomography for coronary stents imaging high-voltage (140-kVp) prospective ECG-triggered versus standard-voltage (120-kVp) retrospective ECG-gated helical scanning. J Comput Assist Tomogr 37:395–401
25. Menke J, Unterberg-Buchwald C, Staab W, Sohns JM, Seif Amir Hosseini A, Schwarz A (2013) Head-to-head comparison of prospectively triggered vs retrospectively gated coronary computed tomography angiography: meta-analysis of diagnostic accuracy, image quality, and radiation dose. Am Heart J 165:154–163 e153
26. Andreini D, Pontone G, Bartorelli AL et al (2011) High diagnostic accuracy of prospective ECG-gating 64-slice computed tomography coronary angiography for the detection of in-stent restenosis: in-stent restenosis assessment by low-dose MDCT. Eur Radiol 21:1430–1438